ME160 Final Project Report

Ram-Air Turbine Blue Team

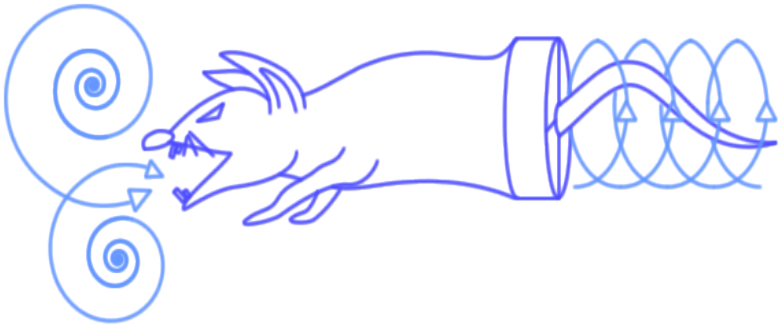

Stephen Clark David Hall

John Kearney Sebastian Liska

Advisor: Dr. Kielb

April 22, 2008

Abstract

The goal of the RAT Blue Team was to design and produce a functioning ram air turbine (RAT) for the Spring 2008 ME160 Mechanical Systems Design class. The project encompassed several objectives, including maximizing RAT efficiency and generating more power than competitors. A ducted fan design was fabricated using a combination of rapid prototyping and shop machining, and structural and vibrational analyses verified the integrity of the design. The completed RAT was installed in a wind tunnel for testing and power generation. Performance results and the success of the project are discussed, possibilities for improvement in some areas are offered, and the value of the overall experience is observed.

1 Project Definition

1.1 Mission Statement

The RAT Blue Team was to develop a ram air turbine capable of consistently outputting power while operating in a wind tunnel and to beat the RAT White Team in a competition of overall performance. The project was to include the complete design, construction, and testing of the RAT, and all components of the project were to be completed in abidance of the Duke Community Standard. The project was to emphasize teamwork and cooperation, the application of engineering knowledge acquired in prior classes, and foresight in project planning.

1.2 Goals

The following goals outline the quantitative benchmarks that the Blue Team sought to achieve. First, the RAT power output was to be optimized for approximately 100 ft/s airspeed though it must be capable of operation between 0 and 100 ft/s. It must operate at a minimum of 25% efficiency (based on the theoretical Betz Limit, to be discussed later) and employ a mechanical brake. Finally, all design, manufacturing, assembly, and testing was to be conducted within the confines of a budget of $1000. These goals were imposed to ensure that the Blue Team achieved the criteria set forth of the mission statement in particular, the Blue Team's RAT must exhibit performance superior to their competition. Therefore, the primary customer for this device is the competition's judges.

Beyond the scale of the competition, the Blue Team's RAT was to improve upon current commercial ram air turbine designs. RATs are first and foremost emergency devices. In the event of complete engine failure, a commercial RAT will deploy from the fuselage of an airplane and provide emergency power for navigation, avionics, and electronically-controlled landing gear systems. In such an event, a sufficient and reliable power supply is crucial. Thus, continuous improvement of RAT products ensures the safety and peace of mind of the public, who may rely on this device in an emergency situation. The Blue Team endeavored to develop a RAT with higher efficiency and simpler manufacturability than current designs. If such a design were constructed, the Blue Team would explore its marketability; in this case, they would conduct more exhaustive research as to the RAT's potential customers and contact current ram air turbine manufacturers (discussed below).

2 Information Gathered

In order to maximize productivity in the semester allotted, the team improved upon current designs rather than re-inventing the wheel. Multiple sources informed the Blue Teams RAT design, including a patent search, an investigation of existing products, consultation from experts in the field of aerodynamics and propulsion, and a survey of an engineer working for a well-known ram air turbine manufacturer.

2.1 Patents

Many devices harness wind power to generate useful work. As far back as the 1st century A.D., windmills have capitalized on wind to drive crankshafts for wells. In 1944, the modern wind turbine was issued a patent in the United States (Patent No. 2,360,792). This design contained complex electrical components and was capable of being adapted to many different engineering situations. An improvement upon this and a novel design in its own right, the air-powered impeller (Patent No. 2,550,229) with variable-pitch blades and speeds up to 4000 RPM was later designed to generate power for glider tow reels (Figure 1).

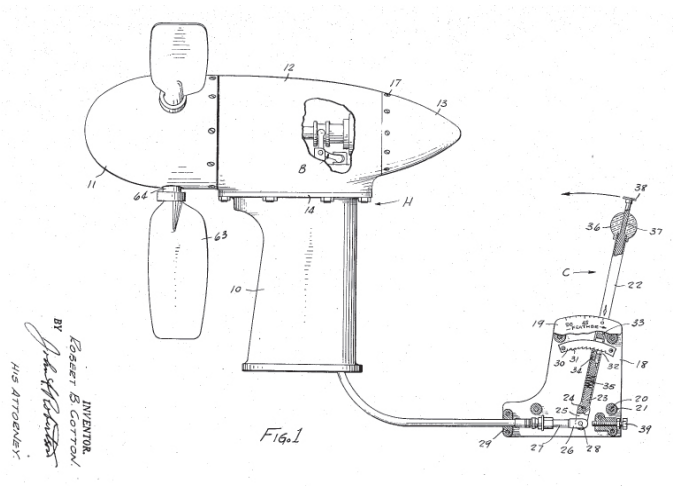

Figure 1: Air-Driven Impeller

These products and innovations like them lead to the air-driven power unit (Patent No. 2,874,787) in which airflow was used to generate electricity and

operate a hydraulic pump. With this technology in place, the modern and complex ram air turbine (Patent No. 5,249,924) was patented by Southwest Aerospace Corporation in 1993 (Figure 2). Since then, many modified designs have been patented for specialized usage. For example, the Low Drag RAT (Patent No. 6,270,309) by Ghetzler Aero-Power consists of a ducted turbine for a generator cooling system with variable-length external fairings and is intended for high speed (transonic or supersonic) applications. The design demonstrates the complexity and capability of modern turbines and inspired the Blue Team to seek an easily-manufactured solution.

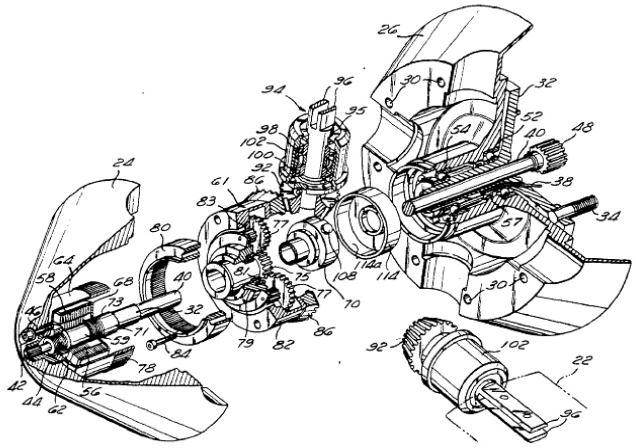

Figure 2: Modern Ram-Air Turbine

2.2 Existing Products

A search of existing turbine products also yielded advice for the Blue Teams design. From Hamilton Sundstrand, the company responsible for designing the

Airbus A380s RAT (Figure 3), the Blue Team gained an appreciation for the a RATs size-to-power ratio. The A380s RAT, for example, has 1.63m diameter blades, weighs approximately 180 kg, and generates 70kW of emergency power (a large portion of the weight is accounted for by the deploying/stowing mechanism). This information provided a frame of reference for the Blue Teams RAT.

Figure 3: Hamilton-Sundstrand Airbus A380 RAT

By reviewing the products by Ghetzler Aero-Power, the Blue Team gained a grasp of the range of applications (and subsequent range of design options) in which RATs are used. Ghetzler makes a low-speed (80-90 knots), low-power (750W), small (11.4 kg) turbine specifically for unmanned aerial vehicles (Figure 3). However, the size, power, and weight of the high-speed RAT (up to 40kW),

shown in Figure 4 and mentioned above,s is much different. It is evident from their differences that the conditions in which the RAT will be used greatly affect its design.

Figure 4: Ghetzler Aero-Power high-speed low-drag RAT

2.3 Expert Consultation

Because testing conditions were to be specified by Dr. Kielb, the Blue Team consulted several experts in the field of aerodynamics and propulsion to gain specific and detailed knowledge of RAT performance. First, through a series of lectures and discussions, Dr. Kenneth Hall described the theory behind turbomachinery propulsion. Based on Actuator Disk Theory, the Betz Limit (stating that the maximum coefficient of power a wind turbine can extract from moving air is 16/27), and the Goldstein Circulation Theorem, Dr. Hall recommended a two- or three-blade propeller design for the RAT. To this end, Dr. Hall directed

both the Blue and White Teams to propeller-design code written by Dr. Drela at MIT.

In contrast, Dr. Jon Protz suggested that the Blue Team pursue a front-mounted ducted rotor-stator combination for two reasons. First, two team members had completed Dr. Protzs Rockets & Gas Turbines course and had experience designing such turbines (including calculating turbine blade angles). Second, Dr. Protz argued that a rotor-stator combination reduces induced drag losses in exchange for viscous losses, resulting in a larger efficiency for the ducted design.

Dr. Robert Kielb, the Blue Team's advisor, agreed with the potential of a ducted rotor-stator design; however, he contested that a rear-mounted rotor-stator would perform better than a front-mounted design. As air moves through the rotor on a front-mounted design, the cross-sectional area of the air passage constricts (because the blade height decreases) and creates an adverse pressure gradient, which damages efficiency and thus performance. In a rear-mounted design, air passes through an expanding area and no adverse pressure gradient is created.

Justin Jaworski, a Ph.D. candidate in Duke Universitys Mechanical Engineering Department, advised that the Blue Team exercise caution in all designs. He noted that power loss in the ducted rotor design arises largely because of a non-zero tip clearance between the rotor and stator duct. If the Blue Teams manufacturing technique could not minimize this distance, Justin counseled, they should remove the stator and pursue a propeller design similar to the one recommended by Dr. Hall. The differences between the rotor-stator and pro-

peller designs can be seen in the Blue Teams CAD drawings in Figure 5.

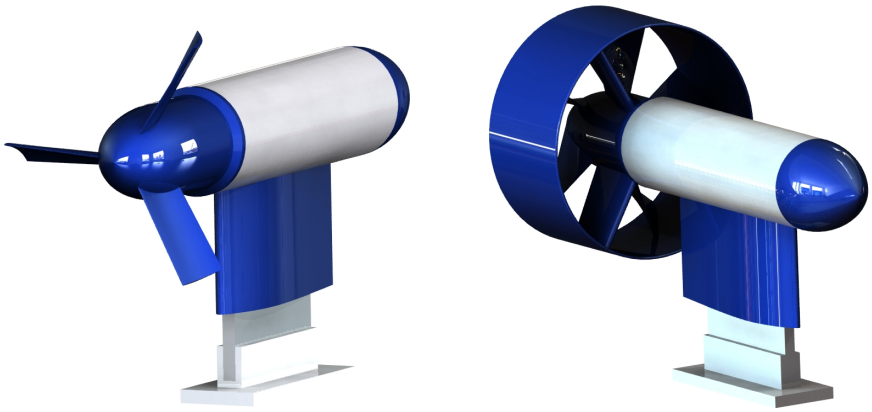

Figure 5: RAT Propeller design on left, and rotor-stator design on right

To determine the capabilities and limitations of the manufacturing equipment available, the Blue Team sought the advice of Pat McGuire and Milan Simonivic. Their recommendations lead to the decision to rapid prototype the rotor, stator, and nosecone of the RAT. Based on the resolution of the 3D printer, Pat and Milan advised extra support for the prototyped parts, allowing the blades to be thicker and more precisely machined. Pat and Milans advice and experience were also invaluable during other manufacturing and assembling procedures.

2.4 Industry Survey

In order to clearly define the areas of RAT design that required the most attention, a survey was sent by the RAT White Team (who shared the results

with the Blue Team) to David Bannon, an engineer with Hamilton Sundstrand. The results, shown in Figure 6, emphasized power output and stowability for a commercial RAT. Combined with the above sources of information gathered, the survey provided the Blue Team with sufficient direction to step into the concept generation phase of their RATs development.

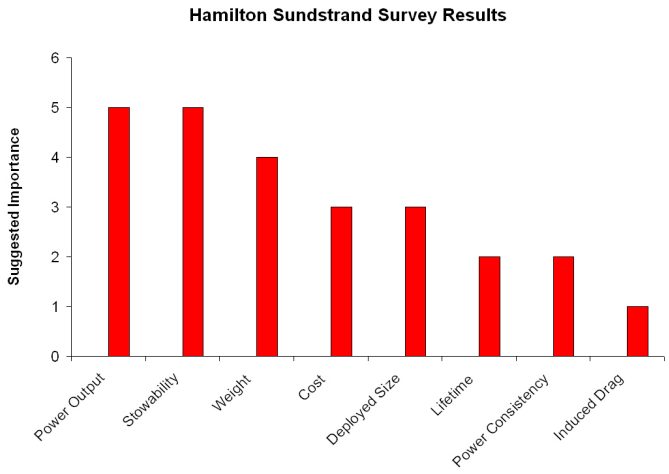

Figure 6: Pareto diagram of survey results received from David Bannon

3 Concept Generation

3.1 Product Design Specification

The Product Design Specification (PDS) guides the development procedure from design to testing by outlining the requirements and goals of the project. Most importantly, the PDS includes the teams mission statement, performance goals, size and weight restrictions, functional requirements, customer requirements,

competition procedures, safety aspects, and testing goals. The PDS is a living document, implying that it may (and should) be continuously updated throughout the course of the products development. The Blue Teams full PDS may be found in the Appendix.

3.2 QFD - Quality Function Deployment

Quality Function Deployment (QFD) is a concept generation process that emphasizes the customers wants and needs. Rather than minimizing defects in a product, QFD balances the customers requirements with the design requirements to maximize the quality and desirability of the product. For the Blue Team RAT, the QFD helped clarify the benefits of a rotor/stator over a propeller design and compared some of the survey recommendations with ease of manufacturing. Through the QFD, the team decided on a horizontally orientation, a blisk (blades and hub are one piece) over detachable blades, a nacelle surrounding the blades, no gearbox, and a rubber braking mechanism. The QFD is presented in the Appendix.

3.3 TRIZ Theory of Inventive Problem Solving

In 1946, Genrich Altshuller and fellow researchers completed their description of a creative process, dubbed TRIZ, for resolving contradictions in engineering. Reportedly based on the survey of over a million patents, the TRIZ tool identifies 39 parameters that designers seek to improve and offers 40 inventive principles to surmount potential problems. A common example of its usage: if an engineer

desires a stronger material yet cannot suffer the extra weight of heavier metal, a TRIZ analysis may recommend the use of a composite (which is both light and strong) instead. When TRIZ is used in conjunction with QFD, an engineer can identify customer and technical needs, then resolve any contradictions between the two.

Based on design specifications and the QFD, the Blue Team sought to improve the power of the RAT without increasing the complexity of the design. As mentioned above, an easily-manufacturable design was highly desirable for the team. The TRIZ analyses suggested four principles:

- 19: Periodic action – instead of continuous action, use periodic or pulsating actions
- 20: Continuity of useful action – eliminate idle or intermittent actions in the device
- 30: Flexible shells and thin films – use flexible shells instead of three-dimensional structures
- 34: Discarding and recovering – discard objects after they have completed their purpose

While none of these principles directly solved the teams dilemma, number 30 did spark ideas about the RATs structure. To reduce weight without reducing power, the rotor and stator designs were modified so that the rapid prototyper would create hollow components rather than solid ones. This decision not only reduced the weight of the teams RAT, but it also reduced the volume of plastic

consumed by the rapid prototyper (a crucial concern if the design were slated for mass production). While TRIZ was not directly responsible for the decision, it was a helpful and useful resource in the development process.

4 Product Architecture

4.1 Prototype I - Aft Rotor/Stator

After a significant amount of consultation with different professors, graduate students, and group meetings, the Blue Team came up with three different design concepts. The first (and primary) concept was recommended to the team by its mentor, Dr. Kielb. The concept design used an aft mounted rotor-stator assembly to generate power. The pros to a rotor stator design are that there is low induced drag, the RAT is cylindrically compact, and the principles behind rotor-stator design were familiar to the group because of prior experience with rotor-stator design. It should also be noted that this design was especially appealing because many of the RATs found commercially were propeller RATs, so part of the challenge (and appeal) of this design would be exploring a relatively unfamiliar concept. The cons associated with this design are the presence of high viscous drag, the need for tighter tolerances between the rotor and stator, and the added weight associated with using a stator (rather than a rotor / propeller all by itself). An exploded view of the primary concept is included in Figure 7.

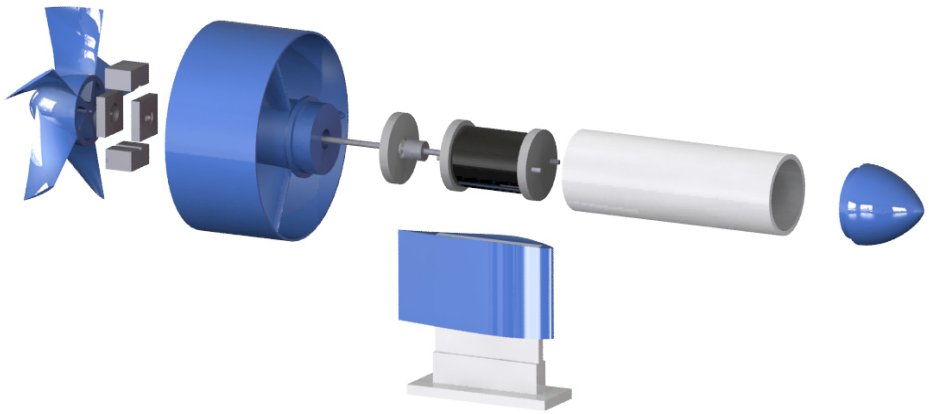

Figure 7: CAD Exploded View of Design Concept I - Rotor-Stator

4.2 Prototype II - Propeller

The second design was recommended to by Dr. Kenneth Hall. Dr. Hall recommended a forward mounted propeller, similar to the propeller on the front of many small airplanes. This propeller concept is good because it has low viscous drag, low weight, and the total volume occupied is relatively small compared to a complete rotor-stator assembly. However, propeller systems have high induced drag, and, most importantly, the methods for solving the propeller equations were complicated and unfamiliar to the team at the time this concept was being explored. A CAD representation of the original propeller design can be seen in Figure 8.

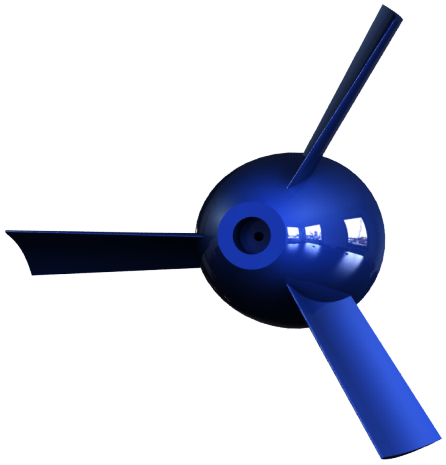

Figure 8: CAD of Design Concept II - Propeller

4.3 Prototype III - Forward Rotor/Stator

The third and final concept was recommended by Dr. Protz. This design concept was another rotor-stator design, just mounted on the front rather than on the rear of the RAT. This third design concept had all of the pros and cons of the aft mounted rotor. In addition, it would offer a larger cross-sectional area for getting air into the RAT. Ultimately, however, the adverse pressure gradients created by the geometry of the rotor hub at a forward orientation, outweighed the increased area associated with mounting the rotor-stator on the front of the RAT. Figure 9 shows a cross-section of this design.

It should be noted that all three of these concept call for the same internal

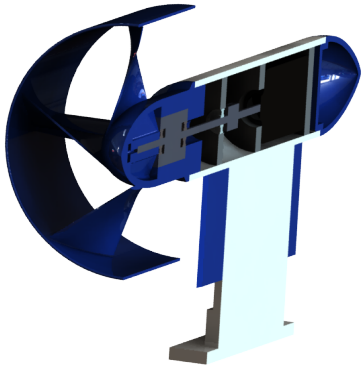

Figure 9: CAD of Design Concept III - Front mounted Rotor/Stator

skeleton, support structure, motor specifications, and have the added benefit of being cheap to produce. An obvious benefit of having these three designs work in the same skeleton and support mechanism is that a final decision about which design concept to pursue does not need to be made until a more thorough analysis is completed.

It was also presumed that the rotor, stator, and propeller would be generated using the Mechanical Engineering Departments rapid prototyping machine; ABS material is obviously much weaker than aluminum or steel, but manufacturing the blades out of metal is too difficult and expensive for the scope of this project.

5 Design Analysis

5.1 Governing Equations

The most complicated component of the design is the rotor-stator assembly, specifically the blades. Had the team pursued a design using a propeller instead, the design for those would also be the most difficult, mathematically intensive part of the project. The rotor-stator design was chosen at the start in the interest of time. By the time the team had learned enough about propeller theory from Dr. Hall to design a propeller, a motor that would not spin fast enough to take advantage of the propeller design had already been purchased, and so the team decided to no longer pursue the propeller option.

One benefit of the rotor-stator design over the propeller is that the math is relatively simple. Where the propeller design involved the solution to a complicated partial differential equation, the design of the rotor and stator blades entails matching the geometries of the two components, so the flow in the absolute frame (as opposed to the relative frame seen by the rotor) flows smoothly when the rotor is spinning at operating speed. Two of the members of our group had taken Dr. Protz's course on Rockets & Gas Turbines, so had no new material to learn, and could immediately begin a design modeled after the turbine section of a gas turbine engine.

The essential equation for the design was the Euler Turbine Equation:

$$P = T\omega = \omega \dot{m} \Delta (v_{tan} r) \tag{1}$$

Where P is power generated by a turbine, T is the torque applied, ω is the angular velocity, $\dot{m}$ is the mass flow, and $\Delta(v_{tan}r)$ is the change from the front of the rotor to the back of the product of the tangential velocity and radius. Using the known quantities of the problem (diameter of the turbine, flow velocity, and expected power output from the Betz Limit), the change in tangential velocity across the turbine was determined. Then, matching flow geometries at the blade hub, blade tip, and the mean-line, the team was able to create blades with quadratic camber, and blade angles that varied with radius, to produce a uniform torque – so as not to create any undue stress on the blade – and also to spin at the desired rotational velocity given the predicted wind velocity. See Appendix for spreadsheet detailing the described design computations.

The relatively simple design plan allowed for the blade geometries to be ready very early in the semester, and also made them easy to import to SolidWorks for ultimate fabrication on the 3D printer, and ANSYS for Finite Element Analysis.

5.2 ANSYS Analysis

The majority of the rotor-stators detailed analysis was performed in ANSYS, testing on the model of a single blade, constrained in all three degrees of freedom at the hub. The capabilities of ANSYS allow for calculation of steady-state stress and displacement, modal analysis to predict resonant frequencies of the blades, as well as statistical analysis, which will be discussing in the following sections.

5.3 Steady-State Analysis

The teams first concerns were that the blades will survive the rotational speeds the turbine was designed for and that they will not deform more than the space between the rotor and the housing. Both these analyses were done fairly quickly in ANSYS. First, the model was built, using the blade geometries computed using the Euler Turbine Equation (essentially, the airfoil shapes at the hub and the tip of the blade were imported, and then the area between was filled in to create the volume of the entire blade). Then the hub of the blade was constrained in all three dimensions, and a centrifugal force for the design speed (1,980 RPM) was added. The model was meshed using 10-node tetrahedrons and assumed the ABS material was isotropic and elastic, using the properties in Table 1. The analysis took a matter of minutes, and at the end, the displacement and stress on every element was known.

Elastic Modulus	236,000 psi
Poisson's Ratio	0.37
Specific Gravity	1.05

Table 1: Material Properties of ABS

The max stress occurred at the hub of the blade at the trailing edge. This is to be expected, since the trailing edge is the thinnest part of the blade and the hub has the largest centrifugal forces on it, due to the fact that the entire mass of the blade is pulling outward. The magnitude of the stress was 1,588 psi, well

below the ultimate tensile strength of ABS (3,200 psi).

The max displacement occurred at the tip of the blade at the trailing edge. This happens in part because the centrifugal force tends to untwist the blade, and the twisting occurs mostly in the trailing three-fourths of the blade. The magnitude of the displacement in the radial direction was 0.044976 inches, small enough that the team did not need to worry about the blades applying a dangerous amount of force on the casing and vice versa.

5.4 Modal Analysis

ANSYS was also used to obtain the natural resonant frequencies of the blade. If some interaction of the blades with the motor, shaft, casing, or air (coming from the stator guide vanes) should occur very close to one of the natural frequencies of the blade, a resonance could start that could ultimately destroy the blade, and possibly cause injury people or equipment.

Since the resonant frequency of the blade will increase with the angular velocity, the modal analysis was done twice, once at zero angular velocity, and once at design speed (1,980 RPM). Frequency increases proportional to the square of angular velocity, so the two sets of frequencies will allow the prediction of the natural frequencies at any speed.

The modal analysis took somewhat longer than the static analysis, and took increasingly longer depending on the desired of number frequencies. The team started with the first five, with the option to run the analysis again if there still might be more natural frequencies in a range with which they were concerned.

The first five turned out to be more than needed, as only the first two modes were actually low enough to conceivably be of any concern. The results for both the static and spinning simulations are given in Table 2.

	Static	Spinning
1st Bending Mode	130.44	136.70
2nd Bending Mode	401.61	406.34
1st Twising Mode	573.48	575.04
3rd Bending Mode	1016.8	1020.3
2nd Twisiting Mode	1206.6	1207.4

Table 2: Natural Frequencies (in Hz) of single blade, first 5 modes

5.5 Campbell Diagram

A useful analysis tool in the aircraft engine industry is the Campbell diagram, which plots frequency vs. rotational frequency. The curves for the vibrating frequency of a blade for the computed modes are plotted as a function of rotational speed (in RPM). Then engine order lines straight lines through the origin with integer slope are plotted on top. These lines represent forcing functions that could happen once, twice, three times, etc. per engine (or in this case, turbine) revolution. The analysis considered up to 15 engine order lines because the rotor had five blades and the stator had three blades. Since the units for frequency were rad/s and the units for angular velocity were RPM, the slopes were actually N/60 where N is an integer. The Campbell diagram for our blade

is shown in Figure 10.

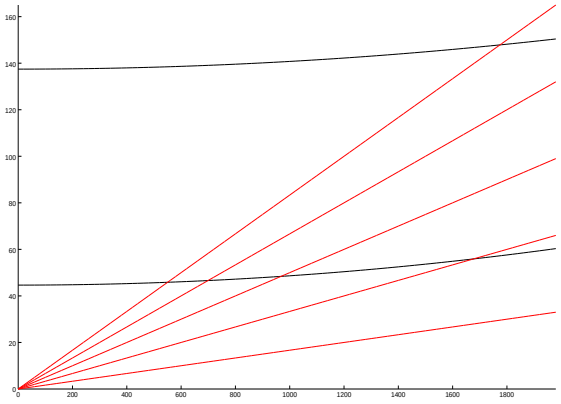

Figure 10: Campbell Diagram for one blade (with 1,2,3,4,5, and 15 engine order lines)

From the diagram, one can see there are two frequencies within the testing range that could be troublesome. One near 1600 RPM, from the fifth and fifteenth (of interest because the rotor has five blades and the stator has three) engine order lines, and another near 2050 RPM. Knowing this, the team was careful to watch for resonances near these speeds during all phases of testing, being sure to ease off or push through if a resonance seemed to be building.
In retrospect, the team should have also performed similar analyses on the stator and rotor housing, since large resonances occurred in the housing during testing. By being vigilant during the tests, though, the team was able to recognize resonances and avoid dangerous instabilities.

5.6 Statistical Analysis

One of the biggest uncertainties in the project was the material properties of the ABS plastic used by the 3D printer. Upon inspection of the printed rotors, the structure of each individual blade seemed to be dependent on its orientation during printing, since the printer can only move along two axes. As a result, the density and elastic modulus must have some inherent variability. The team decided to determine how sensitive the results of the previous analyses (stress, deformation, and resonances) would be to variation in material properties.

Originally, the analysis was to be done in ANSYS using the built in Probabilistic Design System (PDS). However, the process for running PDS is very complicated, and is more suitable to models much simpler than the RAT. Also, because all PDS does is run a normal analysis iteratively with random input variables, a simpler sensitivity analysis using only a few points can be performed. Finally, the team did not have enough documentation about the ABS material to make an informed decision as to the distribution of the material properties that could occur randomly.

Ultimately, the team ended up simply performing the same tests as before, only using different permutations of values for density and elastic modulus, calculating new values for maximum displacement, maximum stress, and vibrational frequencies. Not knowing how widely distributed the material properties are, a conservative estimate was made that both the density and elastic modulus could both range from half the nominal value to double the nominal value. Nine tests were conducted, using permutations of the maximum, minimum, and nominal

values of density and modulus. Since this range distribution was unknown, a safe guess was that it is a uniform distribution, and any of the outcomes are equally possible.

The static analysis yielded results tabulated in Table 3. Since the maximum stress is proportional to density, and the maximum displacement is proportional to the ratio of density to modulus, the case of half density has an even higher factor of safety than the nominal value. At the higher density, the stresses and displacements are dangerously close to the ultimate tensile strength of the material and tip-gap clearance of the rotor, respectively. Viewing that these extremes (double nominal value) were unlikely (the density seemed to be lower than normal on some blades, if at all), the team decided to proceed, but to do so cautiously.

Instead of doing the full modal analysis nine times, the original data was used

	0.525	1.05	2.10
118,000 psi	794.176 psi 0.092517 in.	1588 psi 0.185032 in.	3177 psi 0.370068
236,000 psi	794.176 0.046259 in.	1588 psi 0.092517 in.	3177 psi 0.185032 in.
354,000 psi	794.176 psi 0.030839 in.	1588 psi 0.061678 in.	3177 psi 0.123356 in.

Table 3: Maximum displacement and stress with changes in Elastic Modulus and Specific Density

and the fact that the frequency is proportional to the square root of the ratio of the elastic modulus to the density to come up with a range of material property-dependent frequencies. The results for the first two modal frequencies are given in Table 4.

From the table, it is obvious that the frequency can vary widely with changes

	0.525	1.05	2.10
118,000 psi	130.44	92.235	65.22
	401.61 in.	283.98	200.80
236,000 psi	184.47	130.44	92.235
	567.96	401.61	283.98
354,000 psi	225.93	159.76	112.97
	695.61	491.87	347.80

Table 4: First and Second mode frequencies (in Hz) with changes in Elastic Modulus and Specific Density

in the material properties. This becomes more obvious if a Campbell diagram is plotted accounting for the several values that the vibrational frequency can take on due to variations in material properties (see Figure 11).

Since variability in material properties creates a wide range of possible speeds of resonance, all the team could do was to be careful during testing, take notice of speeds where we see resonances, and move through them quickly and be ready to shut down should a blade fail due to vibration.

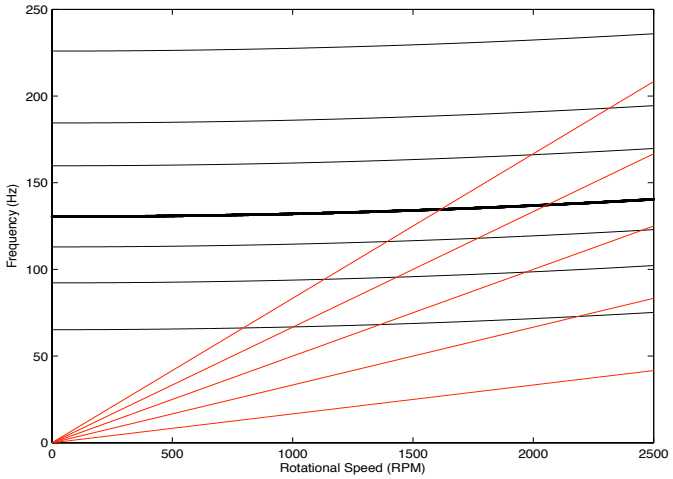

Figure 11: Campbell Diagram for one blade with variability in values for density and elastic modulus

5.7 Other Considerations

Given more time, information, or technology, it would have been desirable to perform a few other analyses. The first of these would be a fatigue analysis, ensuring that the rotor will stand the test of time. A Goodman diagram plotting centrifugal stresses and vibrational stresses would further make sure that our design is safe. The team was unable to include such an analysis due to the lack of information about fatigue in ABS. As mentioned before, it would have been nice to know exactly how the material properties change with respect to printing orientation, allowing perhaps for a full Monte Carlo simulation rather than a basic sensitivity analysis. Lastly, the team would have liked to include some computational fluid dynamic results. With access to or familiarity with a computer program with the ability to perform analysis involving fluid-structure

interaction, such as ANSYS-CFX, Fluent, or the in-house MUSTANG code, the team could have taken into account fluid forces on the blade, and how deformations of the blade affect the flow through the turbine.

6 Prototype Fabrication

The fabrication of the RAT was one of the more difficult and enjoyable portions of the project for the Blue Team. Many of the components were initially designed in SolidWorks to work in all three of the design concepts and therefore the 3-D printing of many of these components was a natural progression from what was designed in our preliminary CAD sketches. In total, the rotor, stator, streamlined support case, and nosecone were fabricated on the 3-D printer, totaling approximately 120 hours of printing.

The most difficult component to print was the rotor-stator assembly (Figure 12).

Figure 12.1 shows the initial attempt at building our rotor. This rotor ended up failing during the print because we had not integrated enough support into the setup of the print job. The support system is vital to a 3-D prints success because it fixes each layer of the ABS in space and does not allow it to move when the next layer is added to the print. Of note is the fact that the first rotor attempt is solid, and was constructed before the TRIZ activity was conducted. Figure 12.2 represents the final version of the rotor. The rotor is significant improved from the initial design in Figure 12.1. The fins are better designed to

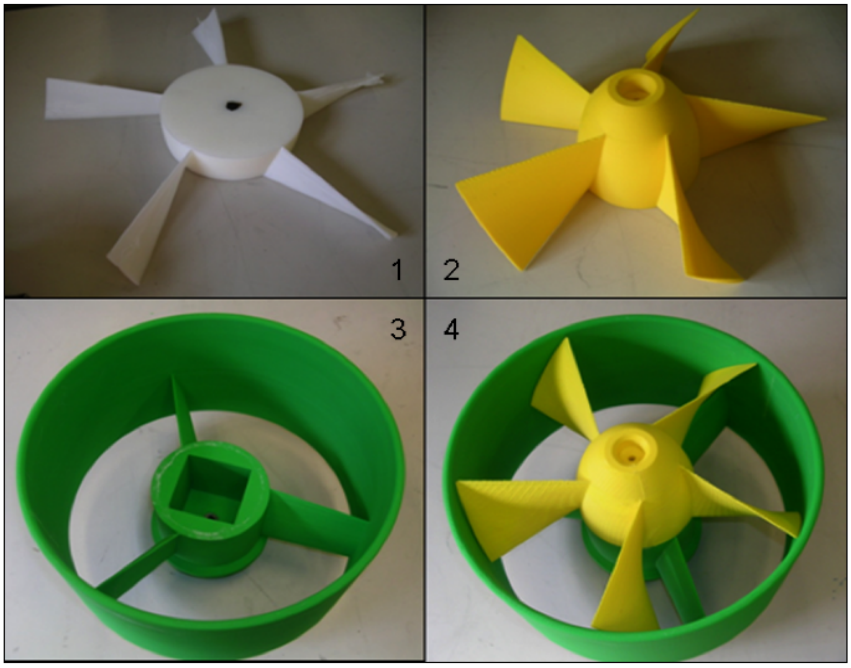

Figure 12: Some of the stages of the rotor-stator build, moving from image 1 to image 4.

account for limitations in print accuracy and resolution and the rotor is hollow with a skeleton to save on weight and total print time. The total diameter of the rotor is designed to exactly equal the diameter of the stator (Figure 12.3) so that tip clearance is at an absolute minimum after sanding. A large tip clearance leads to inefficiencies, which the team obviously tried to avoid in the rotor-stator design.

The complete assembly of the rotor-stator is shown in Figure 12.4. The rotor-stator system is light weight, has small tip clearances, is durable, and although the rotor-stator print totaled 80 hours, its production is fast considering how

long it would have taken to print on a CNC machine or by hand. Figure 13 shows the clearance between the blades of the rotor and the stator.

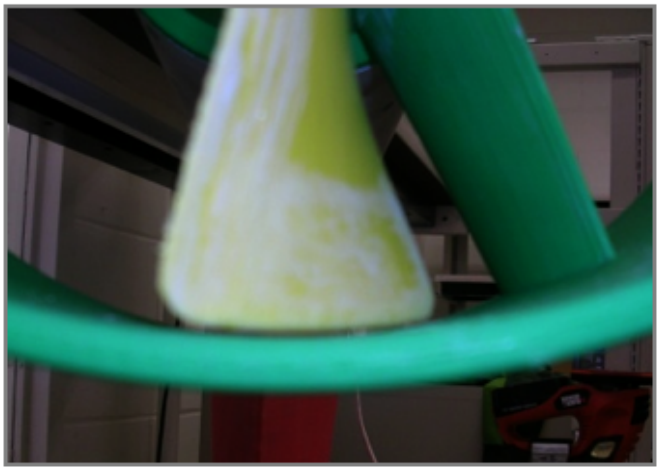

Figure 13: Distance between the Rotor Blades and Stator Cause Inefficiencies

In addition to the rotor and stator, the team also printed an aerodynamic case for the RAT. This case was essentially responsible for covering up the aluminum support system. The design was streamlined so that it would not cause turbulent flow to enter the stator. The Blue Team learned another lesson about the rapid prototyping machine when printing this part. Because the design was not concerned with very tight tolerances (like the rotor and stator builds) this component was built with a coarser technique. It soon became evident that for the rapid prototyping machine, the term coarse truly is coarse; the print missed many important dimensions and a great deal of effort had to be put into making this component work with the rig. None of the remaining prints were completed

on the coarse setting. Figure 14 shows a picture of the aerodynamic shroud that covers our aluminum support structure.

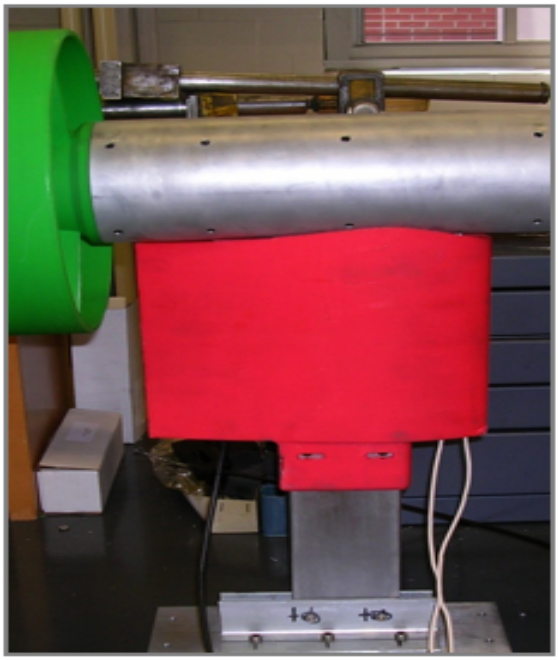

Figure 14: Aerodynamic shroud enclosing support system

Next, the nose cone was printed for our RAT. The purpose of the nose cone was to allow air to smoothly flow around the leading component of the RAT. The nosecone was designed to slide into the aluminum casing (screwed into place) and needed only mild sanding to fit into the tube. Initially when there was concern about the motor overheating, the team considered drilling holes into the front of the nosecone, effectively bleeding cool air into the aluminum tube. Ultimately, holes were drilled directly into the aluminum tube to provide cool

air, and did not have to drill into the nosecone of the RAT. Figure 15 provides an image of the nosecone.

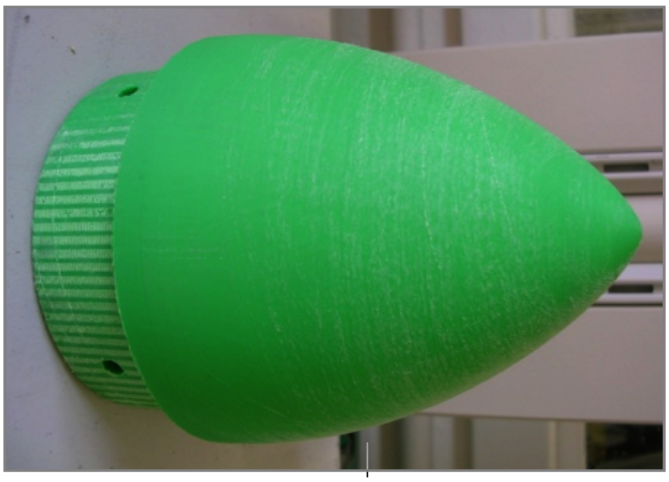

Figure 15: Nosecone made of ABS

Finally, in regards to the plastic printing, the Blue Team would like to thank Duke Universitys Mechanical Engineering Department for donating the materials for the rapid prototyping machine. The RAT assembly was cheap for the team because of this donation, which was estimated to amount to $400 for all of the printing.

In addition to the 3-D printing, there were many other components to be manufactured. The most important of which was the aluminum tube and support that was responsible for containing the innards of the RATs power generation mechanism and supporting the weight of the RAT and any forces associated with the load of the oncoming wind. Figure 16 shows the aluminum casing and

the support, attached with a bead weld on both sides.

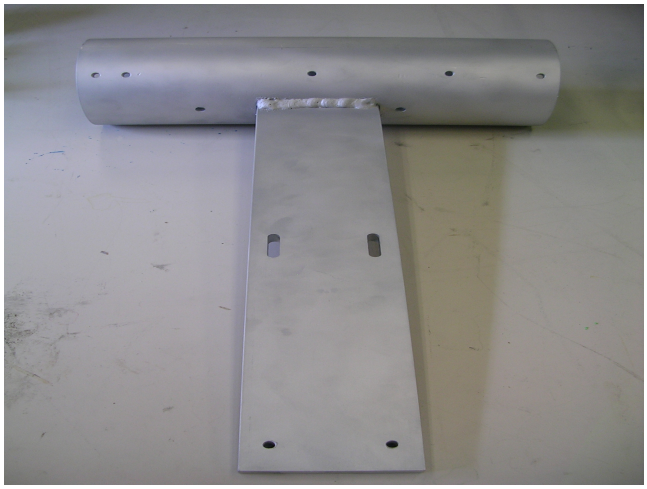

Figure 16: Aluminum Tube and Aluminum Support

The aluminum tube was one of the more difficult components to manufacture. It required a great deal of foresight. Each of the holes pictured in Figure 16 is specifically located to hold one of the internal components (stator, nosecone, motor, delrin disks). Further, because of the difficulties associated with welding two aluminum components together, the weld job was completed by the physics department machinists, who, according to John Goodfellow, had more experience welding aluminum. One difficulty with the aluminum tube was that after it had been welded, it was slightly out-of-round, and was therefore more difficult to work with sliding each of the components in and out of the aluminum during assembly.

Another manufactured component was a sort of internal skeleton for the alu-

minum tube. This skeleton would be responsible for keeping shaft/motor/bearing alignment, and physically supporting each of the components inside the aluminum casing. Figure 17 demonstrates the principles behind how the skeletal disks were used. Delrin, a hard plastic which could be lathed and drilled to proper size, was chosen as the disk material. A total of 3 Delrin disks were made. Two were responsible for holding the motor in place, and the third was responsible for keeping the shaft aligned when it was spinning.

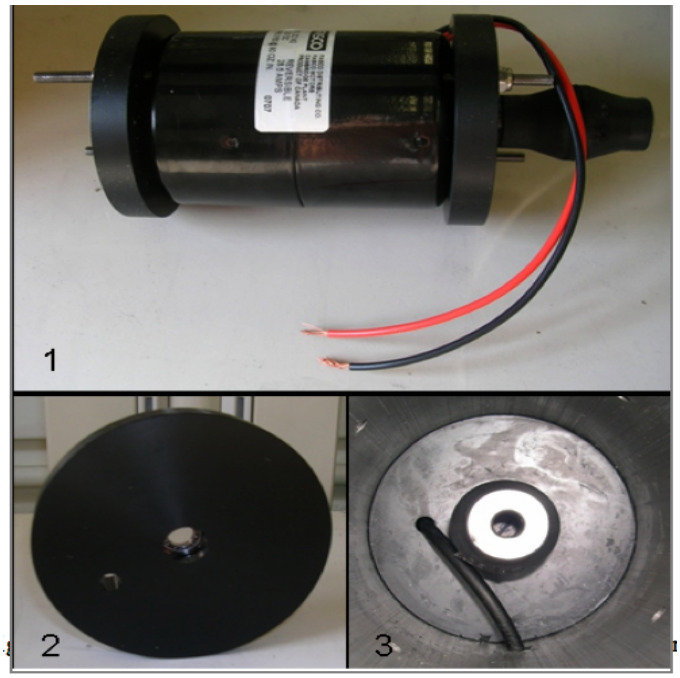

Figure 17: Multiple uses of the Delrin Skeletal Support System

Figure 17.1 shows how the motor was supported by two of these Delrin disks. Figure 17.2 is the third disk used to hold a ball-bearing. This disk also included

a hole on the side for the brake cable. Figure 17.3 shows this third disk, actually inserted inside the aluminum tube, with all of its components assembled.

The brake was one of the more difficult components to manufacture because it had so many small components. The brake consisted of two rubber-coated aluminum plates, which compressed together around the spinning shaft to slow the system. The aluminum plates were separated by a spring, which compressed only when the brake was activated. Brake activation was done with a bicycle brake handle; the bike brake was rigged so that the braking could be done outside of the wind tunnel. Figure 12.3 shows the brake cable feeding through one of the Delrin disks before exiting the aluminum support tube. Also, Figure 18 shows the braking mechanism and its manual trigger.

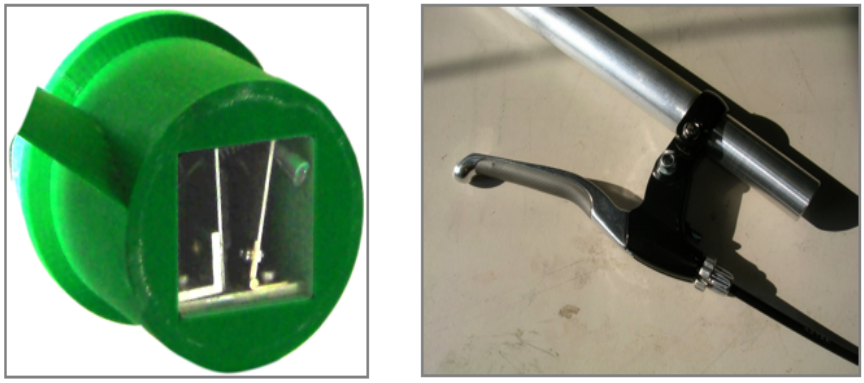

Figure 18: Brake Mechanism and Brake Activation

Preliminary attempts at getting the brake to work were foiled by a weak spring; the spring did not have enough force to push the two aluminum plates

apart after they were compressed. After substituting in a stiffer spring, and fixing some alignment issues, the brake was fully operational.

An essential part of the rig construction was making sure that everything would conform to the wind tunnel. Currently, the wind tunnel is setup to fix things a certain way to its supports and instrumentation. The team had to make sure that the RAT would match these features and meet the size requirements associated with testing in the wind tunnel. Therefore, these requirements were some of the first to be outlined because they were fixed and required design around them.

There were other parts associated with the building and assembly of the RAT. A precision, keyed shaft was ordered to transmit the power from the rotor to the motor, and had centered ball-bearings along its path to reduce shaft vibrations. A coupler bearing connected the precision shaft and the motor shaft; this bearing was very flexible and therefore was able to adjust to misalignment and vibration issues.

A detailed cross-section is included in Figure 19. In this cross-sectional view, one can see each of the components in a full assembly. From left to right Figure 19 shows the rotor, stator, brake, shaft, Delrin disk (with ball bearing), coupler bearing, motor (with two motor mounts), and nosecone.

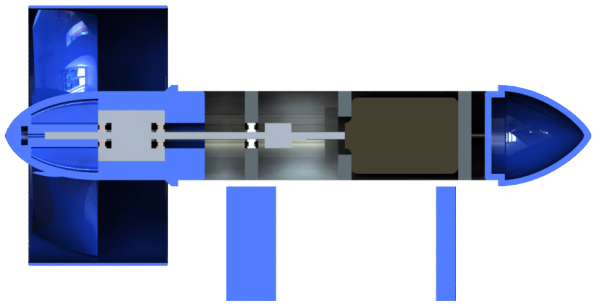

Figure 19: Detailed Cross-Section of the RAT

7 Experimental Setup

7.1 Spin Tests

Before a full test of the RAT took place, the team conducted a series of spin tests to ensure that the rotor would hold together at speed. The first took place in the MEMS fabrication lab, where the first prototype rotor (which was not needed, because it was too big and could not be used for the final design) was attached to the drill press by inserting a short shaft bolted to the rotor into the drill. With some makeshift containment, the team was able to safely spin the rotor up to the maximum speed of the drill press, nominally near 2,000 RPM. The maximum speed of the drill press was later measured by optical tachometer to in fact be 2,906 RPM, higher than any speed the team would run in the wind tunnel.

Once the final prototype was completely assembled, the team performed another spin test, running the DC motor with a power supply to spin the rotor. The RAT was clamped to a table in one of the labs, and the motor was controlled using the power supply from outside, where the team could safely observe the RAT. The optical tachometer was used to measure the angular velocity of the rotor as it spun. The team spun it in both directions, observing resonant frequencies, and making sure the rotor was not damaged. The RAT turned at a maximum of about 2,300 RPM during these tests. Resonances of the rotor housing occurred at 500 RPM and near 1,800 RPM, but they did not seem to grow, so the RAT moved through them without incident. The same test was performed once more the day of the wind tunnel test, with the RAT mounted in the tunnel on the force balance to check one more time that the rotor would survive under test conditions.

The spin tests showed that the RAT was ready for full testing in the wind tunnel. The motor, the shaft, the casing, the stator, and the rotor all survived when the motor was run at design speed.

7.2 Ping Test

One test that was not performed was a ping test. A ping test involves placing a small accelerometer on one of the blades (or the casing, or the shaft, conceivably), and striking it with a small hammer and letting it ring. When a Fourier Transform is performed on the data from the accelerometer, spikes at the resonant frequencies of the object can be seen. This would have been a good test

to refine the predictions of natural frequencies of different components of the RAT. The instruments required for a ping test were available, and given more time, the team would have performed one to have more accurate knowledge of where resonances would occur during the wind tunnel tests.

7.3 Wind Tunnel Test

The important testing occurred in the Department of Mechanical Engineering wind tunnel. During the tests, the team was able to measure the power output, rotational speed, and drag on the RAT at different wind velocities. The tests we performed in the wind tunnel are those which produced the important results to gauge the success of the project, as well as the Blue Teams performance versus that of the White team.

The setup allowed accurate measurement of the voltage, current, and thus power produced by the DC motor/generator, as well as the wind velocity inside the tunnel and the rotational speed of the rotor. The force balance on which the RAT was mounted allowed the team to read the drag on it; however, it was not zeroed at the start, and the team did not know what units of force the machine displays, so the resulting drag values were only good for comparison to the other team. A pitot tube inside the tunnel, just upstream of and above the RAT displayed voltages on a meter, which corresponded to previously tabulated speeds. The optical tachometer was mounted on a vice outside the tunnel, pointed at the rotor to measure the angular velocity. The motor was hooked up to a series of variable resistors, as well as multi-meters to measure the current and voltage.

The emergency procedures were laid out before the start of the test. In case of a failure, the wind tunnel would immediately be shut off by the person taking the power readings, and the mechanical brake would be pulsed by the person taking the velocity readings until the rotor came to a stop. A chicken wire net was installed downstream of the test section the day before the test, so any parts that may have broken off would not damage the wind tunnel. Fortunately, there was no failure, and the emergency procedures never had to be used.

The test plan was a relatively simple one. The wind tunnel was run near three speeds: 50 ft/s, 75 ft/s, and 100 ft/s, respectively. At each speed, the team adjusted the resistance load to try to find the optimum load for maximum power, recording for different loads - the resistance, current, voltage, wind velocity, and rotational speed of the rotor. Once we had taken data for the three speeds defined by the competition, the team continued to increase the wind velocity to determine how much power the RAT could extract at higher speeds. Testing continued up to almost 130 ft/s, with the rotor turning as fast as 2415 RPM, giving a factor of safety of at least 1.22 above the design speed.

The entire wind tunnel test was performed successfully. There were small resonances in the rotor casing at the frequencies previously observed, and by careful manipulation of the wind velocity, the team was able to move through them quickly and safely.

8 Project Results

8.1 Test Results

The results for the wind tunnel test are shown in Figure 20 and tabulated in the Appendix. The RAT produced a maximum of 36.04W (not nearly as much power as hoped for), yet it displayed consistent power curves. The team found an optimal resistance for maximum power at 0.2Ω, near the internal resistance of the motor, as expected. The RAT was able to maintain this consistency even above the design speed. The linear results depicted in Figure 21 indicate that the design maintained robustness despite producing a lower than expected power.

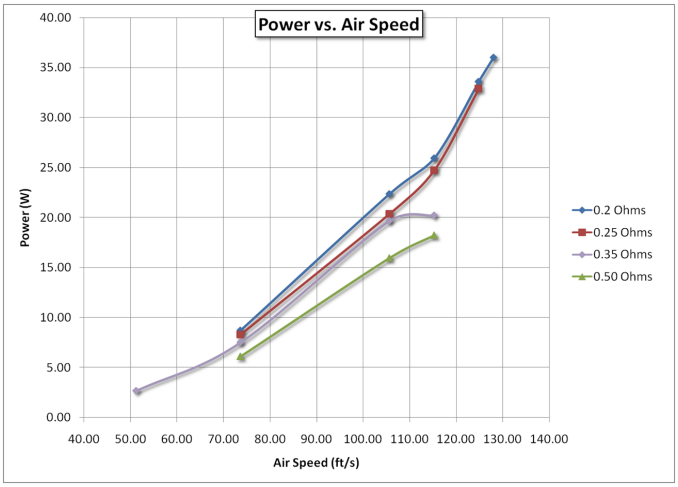

Figure 20: Power vs. Airspeed for various resistor loads

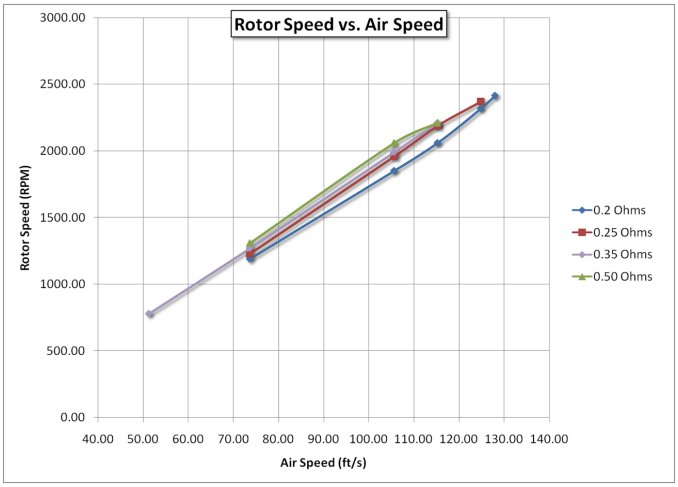

Figure 21: Rotor speed vs. Airspeed for various resistor loads

8.2 Project Time Line

A Gantt chart served as the master record of the teams project timeline. The chart was continuously updated throughout the course of the semester to verify that the project was on schedule. For each component of the teams Conceptual Design, Preliminary Design, Detailed Design, Manufacturing, Data Collection, and Final Stages of the project, the duration and deadline were set. With minimum modifications, the team achieved these deadlines and completed the entire RAT project with time to spare. The teams Gantt chart may be found in the Appendix.

8.3 Final Project Budget

The project had a budget of $1000, sponsored by the Mechanical Engineering department. As previously mentioned in the project fabrication section of this report, the Mechanical Engineering Department also sponsored the material costs (ABS) for the 3-D printing of our rotor, stator, aerodynamic case, and nosecone (an estimated $400 donation). In total, the Blue Team spent a total of approximately $700 dollars of the $1000; a detailed, order-by-order, catalog of our spending is included in the Appendix.

9 Project Conclusions

9.1 Overall Performance

The 2008 ME 160 Ram Air Turbine Blue Team satisfied all design requirements. In building a novel, back-mounted, rotor-stator RAT, the Blue team challenged the paradigms in small commercial RATs. The Blue Team's RAT spun at a maximum of 2450 RPM (a factor of safety of 1.25 beyond designed RPM) and generated 36 W at maximum power. The design further included the safety features required for experimentation (braking mechanism, spin testing) and fulfilled all requirements in concept generation and design analysis. Further, the Blue Team made excellent use of the ABS rapid prototyping machine, generating two integral components (rotor and stator) on the printer. The computational analysis in ANSYS confirmed the experimental results in loading and frequency analysis.

9.2 Discussion

Despite the team's best efforts, the power generated by the RAT during wind tunnel testing was far lower than expected and calculated. In this respect, the team did not fulfill its objective of producing more power than the RAT White Team. However, the Blue Team recognized this design as a prototype and will continue to improve it beyond the competition. The RAT design itself was not flawed - indeed, it's designed rotational velocity matched it's actual rotational velocity at 100 ft/s windspeed exactly. The problems lay in the motor that the team chose. Just prior to the wind tunnel test, the team discovered that the maximum power generation of their motor, when used as a generator, was approximately one-quarter the expected capacity. The team has since ordered a new generator capable of producing approximately 200W of power at the RAT's 1980 RPM design speed.

This project was highly gratifying for all the team members. The application of mechanical engineering principles learned in class, the opportunity for hands-on manufacturing in the lab, and the excitement of following a project to fruition made this semester-long endeavor worthwhile. The Blue Team members leveraged each other's strengths and maintained enthusiasm throughout the project; we are all proud of the result.

10 Acknowledgements

The RAT Blue Team would very sincerely like to thank the following individuals for their support, advice, and encouragement.

- Dr. Kielb
- Pat McGuire and Milan Simonovic
- Dr. Hall, Dr. Protz, and Justin Jaworski
- John Goodfellow